Geometric Heat Equation and Nonlinear Diffusion of Shapes and Images

Benjamin B. Kimia

Division of Engineering
Brown University
kimia@lems.brown.edu

Kaleem Siddiqi

Division of Engineering
Brown University
Providence, RI 02912

Abstract

We propose a geometric *smoothing method based on local curvature in shapes and images which is governed by the geometric heat equation and is a special case of the reaction-diffusion framework proposed by [28]. For shapes, the approach is analogous to the classical heat equation smoothing, but with a renormalization by arc-length at each infinitesimal step. For images, the smoothing is similar to anisotropic diffusion in that, since the component of diffusion in the direction of the brightness gradient is nil, edge location and sharpness are left intact. We present several properties of curvature deformation smoothing of shape: it preserves inclusion order, annihilates extrema and inflection points without creating new ones, decreases total curvature, satisfies the semi-group property allowing for local iterative computations, etc. Curvature deformation smoothing of an image is based on viewing it as a collection of iso-intensity level sets, each of which is smoothed by curvature and then reassembled. This is shown to be mathematically sound and applicable to medical, aerial, and range images.*

1 Introduction

Shapes and images are often perceived as a hierarchical structure of elements. It has been argued that recognition of objects should rely on a representation that captures this structure in a hierarchy of "scale". The basic idea is to introduce a family of shapes, or images, which progressively become simpler. Witkin proposed Gaussian convolution to remove zero-crossings features [51]. Koenderink showed that among the linear operators the heat (diffusion) equation and its associated Gaussian kernel is the only sensible way of smoothing images, by demanding *causality*, *homogeneity*, and *isotropy* [35, 36, 7]. Yuille and Poggio extended this result to two dimensions [52]. See [38] for a smoothing kernel for discrete signals that are modified Bessel functions.

Scale-spaces have also been constructed for shapes. Asada and Brady [6] smooth the curvature function to obtain a hierarchy of features. Mokhtarian and Mackworth [42] smooth the coordinates by a Gaussian filter. Horn and Weldon [24] point to the shrinkage problems of this method and propose instead to filter the extended circular image of the curve with a Gaussian filter. Lowe corrects for the shrinkage problem by inflating the curve proportional to the curvature of the smoothed curve, which indicates how much shrinkage has occurred. Oliensis [44] suggests that this is the case only for small curvature and proposes instead to maintain the low frequencies exactly, while preserving the local nature of the process. Koenderink and van Doorn embed a shape in a morphogenetic sequence based on the Gaussian [36].

Recently, a number of nonlinear diffusion techniques have been proposed to deal with the shortcomings of the linear smoothing techniques. These are summarized in Section 6. Our proposal for geometric smoothing of shapes and images is also nonlinear and is related to the idea of diffusion and the associated Gaussian kernel. To smooth shapes, we deform the boundary along the normal proportional to its curvature. This leads to the geometric heat equation which has many desirable smoothing properties. To smooth images, each iso-intensity level set is considered as a shape, a view afforded by properties of the smoothing process. The curvature deformation smoothing method is related to the linear heat equation smoothing and to anisotropic diffusion. The method has been implemented and applied to several shapes and range and intensity images. In fact, the extension of curvature deformation smoothing of shapes to curvature deformation smoothing of images can be generalized to a combination of constant and curvature deformation, leading to an *entropy scale space* [29] for images. Details of the full space and its mathematical justification will follow in a future paper [48].

The paper is organized as follows. In Section 2 the *shape from deformation framework* as originally presented in [26, 28] and later developed in [31, 29, 30, 34, 33, 32, 5] is briefly reviewed. The focus of this paper is a special case of the reaction-diffusion space, namely, when the shape is deformed only by curvature deformation, giving rise to the geometric heat equation. In Section 3 a number of desirable properties of this nonlinear smoothing process are presented. In Section 4 the idea of smoothing shapes by curvature deformation is extended to the smoothing of images. In Section 5 the connection between the geometric heat equation (curvature deformation smoothing) and the classical heat equation (Gaussian smoothing) is shown. Section 6 shows the connection to anisotropic diffusion. Finally, in Section 7 the process is illustrated on a number of shapes and images, and comparisons are made with some other techniques.

2 The Shape from Deformation Framework

In this section we review a framework for representing two dimensional shape designed to capture its essence in relation to "nearby' shapes. The geometric curvature deformation is a special case of this framework and

provides a smoothing process for shape. We will then extend the idea to smoothing intensity and range images by considering their iso-intensity level sets as shapes.

Robust recognition under variations in the visual scene, such as changes in viewpoint and viewing direction, object movement, growth, *etc.* , demands that shapes be represented not *statically* as a set of unrelated primitives, but *dynamically* in a rich sequence of shapes [36], studied in the context of *deformations* of it. Observing that slight changes in the shape boundary often causes slight changes in the shape itself, we proceed to deform the shape boundary in an arbitrarily general fashion, which is shown to be captured by simpler deformations [26]:

$$\frac{\partial \mathcal{C}}{\partial t} = \beta(s,t)\vec{N}; \quad \mathcal{C}(s,0) = \mathcal{C}_0(s), \tag{1}$$

where $\mathcal{C}$ is the boundary vector of coordinates, $\vec{N}$ is the outward normal, s is the path parameter, t is the time duration (magnitude) of the deformation, and β is arbitrary. This form of deformation embeds certain known techniques in image processing, *e.g.*, $\beta = \pm 1$ gives the prairie fire model of Blum [9]. As another example, when $\beta = \beta(\theta)$, where θ is the local orientation of the curve tangent, *all* algebraic set-theoretic convex morphological operations are embedded, but now in a geometric, differential setting [5]. On the other hand, deformations can depend on the local geometry of the boundary, $\beta = \beta(\kappa)$ [26, 28], and a special representative case is $\beta = \beta_0 - \beta_1\kappa$; see [26, 31, 27, 29, 30, 33]:

$$\frac{\partial \mathcal{C}}{\partial t} = (\beta_0 - \beta_1\kappa)\vec{N}; \quad \mathcal{C}(s,0) = \mathcal{C}_0(s). \tag{2}$$

The space of all possible deformations in this form is spanned by two parameters: the ratio of the coefficients β_0/β_1 and time, t, constituting the two axes of the *reaction-diffusion space*. Underlying the representation of shape in this space are a set of *shocks* [37], or entropy-satisfying singularities, which develop during the evolution. The set of shocks which form along the reaction axis, $\beta_1 = 0$, is indeed the *skeleton* proposed by Blum [9]. Shocks also form along other axes of the reaction-diffusion space and are the key to representing shape. To continue the evolution beyond these singularities, the classical notions of normal, curvature, *etc.* are considered in the *generalized* or *weak* sense by using the concepts of entropy and viscosity solutions [39, 12, 25, 11]. For theoretical as well as numerical reasons the original curve flow is embedded in the level set evolution of an evolving surface [45, 8, 33]. Let the surface be denoted by $z = \phi(x,y,t)$ with the correspondence that the evolving shape is represented at all times by its zero level set $\phi(x,y,t) = 0$. It can be shown that the zero level set of surfaces evolving according to

$$\phi_t + \beta(\kappa)|\nabla\phi| = 0 \tag{3}$$

correspond to the viscosity solutions of (1) with $\beta = \beta(\kappa)$ [8].

The focus of this paper is to study curvature deformation, *i.e.*, when $\beta_0 = 0$. Since β_1 is captured by t, let $\beta_1 = 1$:

$$\boxed{\frac{\partial \mathcal{C}}{\partial t} = -\kappa\vec{N}; \quad \mathcal{C}(s,0) = \mathcal{C}_0(s).} \tag{4}$$

The corresponding surface evolution is

$$\boxed{\phi_t - \frac{(\phi_{xx}\phi_y^2 - 2\phi_{xy}\phi_x\phi_y + \phi_{yy}\phi_x^2)}{(\phi_x^2+\phi_y^2)^{3/2}}|\nabla\phi| = 0.} \tag{5}$$

We now consider curvature deformation in the context of smoothing shapes and images. For shapes, we will construct the surface ϕ from the distance transform of the shape [33]. For intensity or range images it is mathematically valid to directly obtain the surface ϕ from the grey level information, as we shall see in Section 4. Each level set is then "smoothed" by curvature deformation. We now discuss properties of this process in addition to its connection to several standard smoothing techniques.

3 Nonlinear Smoothing by Curvature Deformation

Curvature deformation smoothing exhibits a number of interesting properties:

Order Preserving Smoothing: Curvature deformation evolution (4) is known as the "curve shortening flow" in differential geometry. In the process of curvature deformation disjoint closed curves remain disjoint by an application of the maximum principle for parabolic differential equations [47, 50]. As a result, two shapes, one inside another, will never cross in the process of smoothing; see Section 4 for a more detailed analysis.

Smooth Smoothing: A shape lasts only a finite time under curvature deformation smoothing, due to the order preserving property, since any closed curve can be considered inside some large circle with a finite evolution time (a circle lasts only for a finite time). This finite evolution time under curvature deformation naturally raises three interesting questions: First, must every curve collapse to a point, or can it collapse to a set of points, or segments? Second, if a curve must collapse to a point, will the limit point be round? Third, will the curve develop self-intersections or become singular in the process?

Gage and Hamilton [18, 19, 21] answered these questions for a convex curve and showed that it must evolve to a round point without developing self-intersections or singularities. Grayson [22] generalized this result to show that *any* embedded curve will become convex without developing self-intersections or singularities. To appreciate the significance of this theorem examine the spiral shape in Figure 1 which must evolve to a circular point. We now state the theorem as derived in Grayson [22].

Theorem 1 *Let $\mathcal{C}(s,0) : S^1 \to \mathbf{R}^2$ be a smooth embedded curve in the plane. Then $\mathcal{C} : S^1 \times [0,T) \to \mathbf{R}^2$ exists and satisfies $\frac{\partial \mathcal{C}}{\partial t} = -\kappa\vec{N}$, where $\mathcal{C}(s,t)$ is smooth for all t, it converges to a point as $t \to T$, and its limiting shape as $t \to T$ is a round circle, with convergence in the C^∞ norm.*

Decreasing Total Curvature: A measure of complexity for a shape is the total curvature of its boundary. Total curvature $\bar{\kappa}$ is defined as $\bar{\kappa} = \int_0^{2\pi} |\kappa| g\, ds = \int_0^L |\kappa|\, d\tilde{s}$, where g is the metric (speed), $\tilde{s}$ is the arc-length parameter, and L is the length of the boundary. The following theorem shows that all non-circular embedded curves evolving by curvature deformation (4) have strictly decreasing total curvature. A circle is the only curve for which total curvature remains constant, $\bar{\kappa} = 2\pi$.

Theorem 2 *Let a family of curves satisfy (4) for which $\beta_1 > 0$. Then, if $\kappa_{\tilde{s}}(\tilde{s},t) \neq 0$ for all $\tilde{s}$ and all $t > 0$, $\bar{\kappa}(t) < \bar{\kappa}(0)$.*

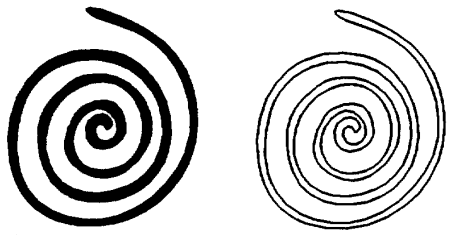

Figure 1: The high curvature end points will move in much faster than the low curvature points in such a way that self-intersections are avoided, keeping the boundaries apart in the process of evolving to a round point!

Proof. The proof is a special case of a general theorem on evolution governed by equation (1) with $\beta = \beta(\kappa)$, which states that the result for general deformations holds when $\beta_\kappa < 0$ [31]. For curvature deformation, $\beta(\kappa(s,t)) = -\beta_1\kappa$, and the condition reduces to $\beta_1 > 0$. Note that for $\beta_1 < 0$ the process is unstable in analogy to the inverse heat equation; see also Section 5.

Annihilation of Extrema and Inflection Points: Another issue of concern is whether new curvature extrema or inflection points can be created in the process of smoothing. The following theorem shows that no new curvature extrema or inflection points can be created. Since the total curvature is strictly decreasing for non-circular shapes, we conclude that existing extrema and zeros of curvature must also disappear in time.

Theorem 3 *Let a family of curves satisfy (4) for which $\beta_1 > 0$. Then, the number of curvature extrema (vertices) is a non-increasing function of time. Similarly, the number of zeros of curvature is a non-increasing function of time.*

Proof. This theorem [34] is based on an application of the following theorem which itself is based on an application of the maximum principle to the following linear parabolic operator [2, 3, 4, 41]:

$$u_t = a(x,t)u_{xx} + b(x,t)u_x + c(x,t)u, \qquad (6)$$

where the coefficients are smooth functions defined on the rectangle $R_T := [x_0, x_1] \times [0, T]$, and $a(x,t)$ is positive. Suppose that u is a classical solution of (6) with $u(x_i,t) \neq 0$ for $i = 0, 1$, and $0 \leq t \leq T$. Let $z(t)$ be the number of zeros of $x \rightarrow u(x,t)$ counted with multiplicity. Then in [2, 41], it is proven that $z(t) < \infty$, and $z(t)$ is a non-increasing function of t. Moreover, at any time t when $x \rightarrow u(x,t)$ has a zero of order $k > 1$, $z(t)$ drops by at least $k - 1$.

The evolution of curvature when the curve evolves by (4) follows $\frac{\partial \kappa}{\partial t} = \kappa_{\tilde{s}\tilde{s}} + \kappa^3$ [31], which by letting $v = \kappa_{\tilde{s}}$ is transformed to

$$v_t = v_{\tilde{s}\tilde{s}} + 4\kappa^2 v. \qquad (7)$$

Using the above theorem on the zeros of linear time-varying parabolic PDEs, we see that the number of vertices (curvature extrema) is non-increasing, as long as $v \neq 0$ for one point, namely, if the curve is not a circle. Circles, however, evolve to smaller circles without creating new curvature extrema. A similar argument holds for flexes (curvature zero crossings); see [34] for details. Therefore,

Corollary 1 *The number of vertices and flexes for a non-circular curve is strictly decreasing; circles have no flexes or vertices and will evolve none.*

Iterative Smoothing: Ideally a smoothing process should be implementable locally and iteratively, with the potential of parallelization. A property that would make this possible is the *semigroup* property. For example, Gaussian smoothing satisfies the semigroup property:

$$[f(s) * K(s,t_1)] * K(s,t_2) = f(s) * K(s,t_1+t_2). \qquad (8)$$

This implies that to smooth by an amount $2t$ one can smooth by t in two sequential steps. There is great computational savings in doing so since the effective width of a Gaussian is much smaller for smaller steps. Similarly, deformation by curvature also satisfies the semigroup property [16].

Theorem 4 *Let $T(t)$ be the operator that evolves an initial curve $\mathcal{C}_0$ to $\mathcal{C}_t$ by curvature, i.e., $\mathcal{C}_t = T(t)\mathcal{C}_0$. Then $T(t+s) = T(t)T(s)$.*

Other Properties: Curvature deformation is the *fastest* way to shrink the length of a curve [20]. The speed of shrinkage of length, among all curves of length L, is slowest for the circle. However, the enclosed area decreases at a constant rate which equals the total curvature of the curve. This shrinkage effect occurs in other smoothing operators and various solutions have been proposed; see for example [40] for a way to deal with Gaussian smoothing shrinkage effects. Alternatively, one can use results suggested by Gage to overcome this effect: he defined an "area-preserving" flow by subtracting the component of the length gradient, $L_t = -\int(\mathcal{C}_t, \kappa\vec{N})\,ds$, which lies parallel to the area gradient, $A_t = -\int(\mathcal{C}_t, \vec{N})\,ds$, where L is the length and A is the area of the curve [20]. This leads to the evolution

$$\mathcal{C}_t = (\kappa - \frac{2\pi}{L})\vec{N}, \qquad (9)$$

namely, the gradient flow of the length functional among curves of a fixed area. All convex curves evolving by equation (9) remain convex and converge to round points in the limit. Although this is not yet shown for simple curves, simple curves remain simple with their isoperimetric ratio decreasing, with circles as the only stationary curves. A second approach to keep the area fixed is also proposed by Gage [20]: magnify the plane by a homothety simultaneously with the evolution, leading to,

$$\mathcal{C}_t = (\kappa - \frac{\pi p}{A})\vec{N} + \alpha\vec{T}, \qquad (10)$$

where p is the support function of C; the tangential component does not change the shape as explained earlier.

In our framework, flows that preserve area, length, and other similar functionals are simply special cases in the reaction-diffusion space, as represented by (2). For example, the area preserving flow (10) is a special vertical axis of the reaction-diffusion space. Note, however, that the length and area measures are *global* and are seriously affected by changes in the scene, *e.g.*, partial occlusion. The fact that such global measures can become variable under visual transformations motivates the use of the full reaction-diffusion space. In this context, the evolution of a partially occluded shape by some ratio β_0/β_1 will match the evolution of the full shape with a different ratio.

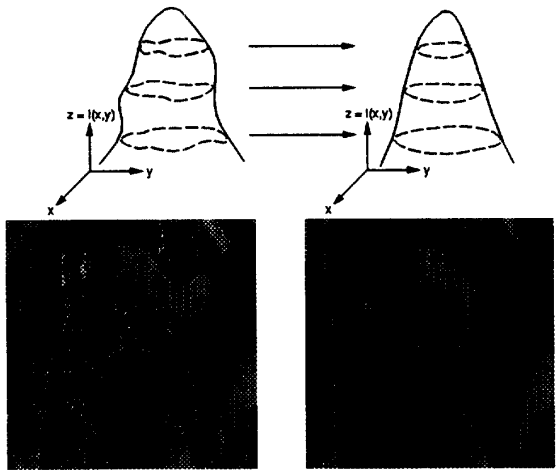

Figure 2: The extension from shapes to images of smoothing by curvature deformation. An intensity image is represented as a surface and each level set is smoothed by curvature deformation. The smoothed image is obtained by superimposing the smoothed level sets. For illustration, we superimpose level set 75 in white on an image (bottom left), and a curvature deformation smoothed version of it (bottom right).

4 Smoothing Images Via Level Set Deformation

To extend curvature deformation to the smoothing of images, recall that curve deformation is implemented as the evolution of a surface which embeds the evolving curve as its zero level set (5). Since any continuous surface can be used, this additional degree of freedom enables grey level intensity or range information to be represented by ϕ. Our view of smoothing images, then, is to smooth each iso-intensity level set by curvature deformation, in analogy to binary shapes, and superimpose the smoothed level sets, Figure 2. However, first a number of essential properties must be established. The first and second theorems allow us to consider images where each iso-intensity level set may have singularities, *e.g.*, corners, disconnected pieces, *etc.* , by viewing the surface evolution in a "weak" sense [39, 13, 23, 37]. The third theorem shows that the smoothing of each iso-intensity contour is independent of the image itself, Figure 6. The fourth theorem shows that the evolution process is order preserving and does not allow iso-intensity level sets to cross. In fact, although iso-intensity level sets may initially share segments in common due to discretization, the fifth theorem shows that these will pull apart after smoothing. The last theorem ensures that iso-intensity level sets never move closer to one another than they were initially. These recent mathematical results provide essential theoretical justification for the extension of curvature deformation smoothing to images.

Consider the parabolic partial differential equation

$$\begin{aligned} \phi_t &= |\nabla\phi| \mathrm{div}\left(\frac{\nabla\phi}{|\nabla\phi|}\right) && \text{in } \mathbf{R}^n \times [0,\infty); \\ \phi &= \phi_0 && \text{on } \mathbf{R}^n \times \{t=0\} \end{aligned} \qquad (11)$$

for the hypersurface $\phi = \phi(x,t)$, $(x \in \mathbf{R}^n, t \geq 0)$, where $\phi_0 : \mathbf{R}^n \rightarrow \mathbf{R}$ is some continuous function such that ϕ_0 is constant on $\mathbf{R}^n \cap \{|x| \geq S\}$, for some $S > 0$. This equation evolves each level set of ϕ according to its mean curvature, at least where ϕ is smooth and its gradient does not vanish. In our case, $n = 2$, (11) reduces to (5). We now restate a number of useful and relevant properties for $n = 2$, which were established in [16] for general n. $\mathcal{C}_0$ denotes a particular level set of ϕ_0 and $\mathcal{C}_t$ is its evolution in time.

Theorem 5 *A "weak" solution to (11) exists and is unique.*

It is important to consider the evolution in the weak sense, in the context of "viscosity solutions" of nonlinear partial differential equations [39, 13]. This allows us to consider shapes that have corners or discontinuities in orientation where, for example, the classical notion of a normal is not well defined. However, we are assured that when the classical solution exists, it coincides with the weak solution:

Theorem 6 *The evolution by curvature (11) agrees with the classical motion by curvature, if and so long as the latter exists.*

Theorem 7 *The evolution of $\mathcal{C}_0$ into $\mathcal{C}_t$ is* independent *of the choice of the initial function ϕ_0.*

This important result stating that the evolution of a level set by its curvature is *independent* of the choice of ϕ_0 underlies our approach to smoothing images. Observe that if we select the image intensity function as the surface ϕ_0, each iso-intensity level set of ϕ_0 will evolve by curvature, exhibiting all the desirable properties detailed in Section 3. This is equivalent to evolving each iso-intensity curve *separately* by curvature, see Figure 6, but with significant computational savings. This approach exhibits properties of anisotropic diffusion for images, see Section 6.

Theorem 8 *If $\mathcal{C}_0$ and $\hat{\mathcal{C}}_0$ are two compact subsets of $\mathbf{R}^2$ such that $\mathcal{C}_0 \subseteq \hat{\mathcal{C}}_0$ then the subsequent evolutions $\mathcal{C}_t$ and $\hat{\mathcal{C}}_t$ of $\mathcal{C}_0$ and $\hat{\mathcal{C}}_0$ satisfy $\mathcal{C}_t \subseteq \hat{\mathcal{C}}_t$.*

It is clear that in the continuous domain, the iso-intensity contours of an image are isolated and non-overlapping. Conversely, for a collection of level sets to represent iso-intensity contours of an image, they too must be non-overlapping. Theorem 8 assures us that the level sets maintain this property during evolution by curvature deformation. We had earlier referred to this property as inclusion order preserving, Section 3. Whereas iso-intensity contours are separated in the continuous domain, in the discrete domain some level sets may partially overlap. Theorem 9 assures us that so long as such level sets do not cross, they will separate in the course of the evolution, Figure 3.

Theorem 9 *Given two initial curves $\mathcal{C}_0$ and $\hat{\mathcal{C}}_0$ such that $\mathcal{C}_0 \subseteq \hat{\mathcal{C}}_0$ but $\mathcal{C}_0 \neq \hat{\mathcal{C}}_0$, their evolutions $\mathcal{C}_t$ and $\hat{\mathcal{C}}_t$ do not coincide for any $t > 0$.*

In fact, Theorem 10 guarantees that two level sets cannot move closer to one another than they were initially.

Theorem 10 *Assume $\mathcal{C}_0$ and $\hat{\mathcal{C}}_0$ are nonempty compact sets in $\mathbf{R}^2$ and $\{\mathcal{C}_t\}_{t>0}$ and $\{\hat{\mathcal{C}}_t\}_{t>0}$ are the subsequent generalized motions by curvature. Then $dist(\mathcal{C}_0, \hat{\mathcal{C}}_0) \leq dist(\mathcal{C}_t, \hat{\mathcal{C}}_t)$ for $t \geq 0$.*

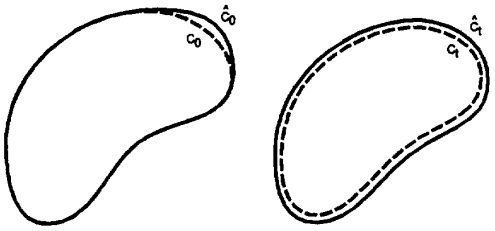

Figure 3: Initially overlapping contours separate during curvature deformation, *i.e.*, if $\mathcal{C}_0 \subseteq \hat{\mathcal{C}}_0$ but $\mathcal{C}_0 \neq \hat{\mathcal{C}}_0$, the two curves will pull apart instantly, even when $\mathcal{C}_0$ and $\hat{\mathcal{C}}_0$ coincide except for a small region [16].

Whereas thus far we have specialized to the case of curvature deformation, a number of the above properties hold for a larger, more general class of geometric parabolic partial differential equations [11]. This includes the evolution of each level set of ϕ by a combination of constant and curvature deformation (2), where ϕ evolves according to (3), with $\beta(\kappa) = \beta_0 - \beta_1\kappa$. In particular, a unique weak solution exists, and the evolution of each level set of ϕ is independent of that of the other level sets. As a consequence, the extension of curvature deformation of shapes to curvature deformation of images may be generalized to a combination of constant and curvature deformation, leading to an *entropy scale space* [29] for images. Examples are shown in Section 7; details will be presented in [48].

5 Connection to the Heat Equation and Gaussian Smoothing

The coordinates of a curve evolving by curvature deformation (4) satisfy $\frac{\partial \mathcal{C}}{\partial t} = \Delta_{\tilde{s}}\mathcal{C}$, where $\Delta_{\tilde{s}} = \frac{\partial^2}{\partial \tilde{s}^2}$, and $\tilde{s}$ is arc-length. Note that this equation is coupled with $|\mathcal{C}_{\tilde{s}}| = 1$, leading to a nonlinear system of equations.

Gaussian smoothing of the coordinates is given by $x(s,t) = x_0(s) * K(s,t)$; $y(s,t) = y_0(s) * K(s,t)$, where t is the extent of the Gaussian $K(s,t)$. Since the Gaussian is the heat kernel, $\frac{\partial \mathcal{C}}{\partial t} = \Delta_s\mathcal{C}$. In the short time, since arc-length is approximately preserved, the two smoothing processes are similar. However, for larger smoothing time, the two processes diverge in effect. Evolutions by $\frac{\partial \mathcal{C}}{\partial t} = \Delta_s\mathcal{C}$ can cause self-intersections, since they place too much significance on elongated features; the remedy is to renormalize for arc-length in each step [43], effectively yielding $\frac{\partial \mathcal{C}}{\partial t} = \Delta_{\tilde{s}}\mathcal{C}$.

A second connection between curvature deformation and Gaussian smoothing is based on "volumetric blurring" [35, 36] where the focus is on the blurring of the region rather than the boundary. In [14] Evans and Spruck show that blurring the signed distance function with a Gaussian kernel of small extent and then thresholding is equivalent to curvature deformation. An intuitive explanation of this result is as follows. The heat equation may be written as $\phi_t = \Delta\phi = \phi_{rr} + \phi_{r'r'}$, where r and r' are any two orthogonal directions. Let r' be the direction of $\nabla\phi$. If we specialize to the case of the signed distance function as ϕ, near the shape's boundary, $|\phi_{r'}| = 1$. Consequently, $\phi_{r'r'}$ is zero near the boundary. Now recall that curvature deformation satisfies (5), $\phi_t = \kappa|\nabla\phi|$. Here ϕ is any continuous surface, including but not limited to the signed distance function, whose level sets evolve by mean curvature. Since $\kappa = \frac{\phi_{rr}}{|\nabla\phi|}$, we have $\phi_t = \phi_{rr}$. Therefore, the approaches of curvature deformation and region blur converge when ϕ is the signed distance function.

6 Connection to Anisotropic Diffusion

A number of linear scale spaces have been introduced to combat noise as well as to hierarchically structure features. Perona and Malik [46] observe a shift in the true location of edges in scale, chiefly due to the homogeneity assumption in standard linear scale spaces. They propose a piecewise smoothing method which aims to localize edges as indicated by the gradient of the image, leading to the anisotropic diffusion equation

$$\phi_t = \mathrm{div}(c(x,y,t)\nabla\phi) = c(x,y,t)\Delta\phi + \nabla c \cdot \nabla\phi, \quad (12)$$

where ϕ denotes brightness intensity. Smoothing at boundaries is turned off by a measure of edge strength: $c(x,y,t) = g(|\nabla\phi(x,y,t)|)$. As a consequence, regions of low brightness gradients are blurred, while regions of high gradient values are not.

Catté *et al.* [10] point out two limitations of the Perona-Malik scheme. First, "noise introduces very large, in theory unbounded, oscillations of the gradient", leading to the enhancement of noise edges, which will then be kept. These edges are in practice filtered by a first stage smoothing, which in turn introduces an additional parameter. The second problem relates to the existence and uniqueness of solutions; pictures close in norm can yield drastically different edge maps. They propose a slight modification where the gradient in $g(|\nabla\phi(x,y,t)|)$ is replaced with a Gaussian smoothed estimate $|DG_\sigma * \phi(x,y,t)|$, leading to

$$\phi_t = \mathrm{div}(g(|DG_\sigma * \phi(x,y,t)|)\nabla\phi). \quad (13)$$

In other words, the initial smoothing of Perona and Malik is now integrated into the scheme. A similar idea is proposed by Whitaker and Pizer [49], where the extent of the Gaussian is itself a decreasing function of time.

Alvarez *et al.* [1] study a class of nonlinear parabolic differential equations specified by

$$\begin{aligned} \phi_t &= g(|G * \nabla\phi|)|\nabla\phi|\mathrm{div}\tfrac{\nabla\phi}{|\nabla\phi|}; \\ \phi(x,y,0) &= \phi_0(x,y), \end{aligned} \quad (14)$$

where G is a smoothing kernel, say the Gaussian, and $g(\xi)$ is a nonincreasing real function which tends to zero as $\xi \to 0$. They then show the existence and uniqueness of the viscosity solution of this equation. Our curvature deformation is related to (14) in that $g(.) = 1$ ($g(\xi)$ does not tend to zero as $\xi \to 0$). However, the theory of viscosity solutions of the curvature deformation, known as the "mean curvature flow", was addressed previously [16, 14, 15, 11], and was numerically demonstrated by Osher and Sethian [45].

To see how curvature deformation preserves edges while smoothing, recall that under this process, $\phi_t = \phi_{rr}$, where r is the direction perpendicular to the image intensity gradient $\nabla\phi$. In contrast to the heat equation, $\phi_t = \Delta\phi = \phi_{rr} + \phi_{r'r'}$, where r and r' are any two orthogonal directions, we observe that curvature deformation ignores the diffusion term $\phi_{r'r'}$ in the direction r' of the brightness gradient, and as such does not allow diffusion across edges [1]. Edge location and sharpness

are left intact since, in effect, the component of diffusion along the gradient has been subtracted off. This is similar to Perona and Malik's approach in that the edges are preserved. However, "noise edges" are not amplified because curvature deformation does not enhance edges. This is the anisotropic diffusion connection.

7 Examples

In this section we discuss implementation issues and illustrate the scheme with several examples. Since curvature deformation smoothes singularities and no new singularities can form, a central difference scheme is sufficient to robustly simulate the process. The numerical scheme for curvature deformation *requires no parameters*. The magnitude of β_1 is absorbed in the time parameter t and only affects the speed of smoothing. The original shape/image is evolved over time, producing a sequence of fine to coarse smoothed shapes/images.

Figure 4 depicts the original shapes and images. Figure 5 compares the curvature deformation of a shape with Gaussian blurring of its region and its boundary, respectively. Figure 6 demonstrates that each iso-intensity level set evolves independently of the original image. The numerical simulation confirms the theoretical results, Theorem 7. Figure 7 illustrates the extension from shapes to images of a combination of constant and curvature deformation, leading to an entropy scale space [29] for images; a spectrum of smoothing processes ranging from the "breaking off" of chunks to the "melting" of less significant features. Figure 8 depicts an application to the medical domain; curvature deformation smoothing facilitates the measurement of the width of the ocular dominance bands by removing the blood vessels that congest them. Figure 9 compares curvature deformation with Perona and Malik's anisotropic diffusion [46] for an aerial image taken from the ARPA RADIUS program.

Acknowledgements This research was supported by NSF grant CDA-9305630. The authors thank Steven W. Zucker for many discussions and Perry Stoll for some of the implementations. The medical images were kindly provided by Michael Stryker from UCSF. The aerial image is from the ARPA RADIUS program.

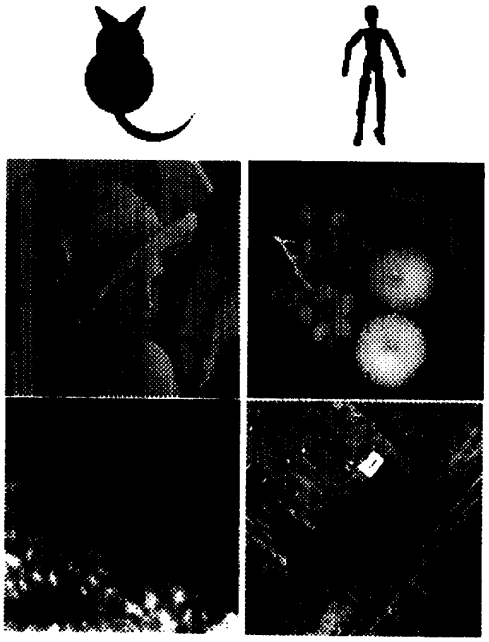

Figure 4: The original shapes and images used for the examples: CAT, DOLL, LENA, FRUITS, BANDS and ROADS.

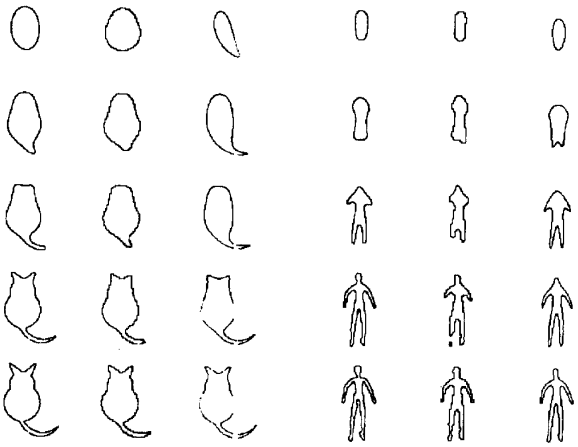

Figure 5: Curvature deformation (LEFT COLUMNS), region blurring (MIDDLE COLUMNS) and boundary blurring (RIGHT COLUMNS). Boundary blurring can place too much emphasis on elongated features, *e.g.*, the tail of the CAT shape; region blurring can lead to topological splits, *e.g.*, the hands and feet of the DOLL shape. Curvature deformation exhibits several desirable properties, in particular each shape becomes round in the limit.

References

[1] L. Alvarez, P.-L. Lions, and J.-M. Morel. Image selective smoothing and edge detection by nonlinear diffusion: II. *SIAM Journal of Numerical Analysis*, 29(3):845–866, June 1992.

[2] S. B. Angenent. The zero set of a solution of a parabolic equation. *J. für die Reine und Angewandte Mathematik*, 390:79–96, 1988.

[3] —. Parabolic equations for curves on surfaces, I. Technical Report Technical Summary reports, 89-19, University of Wisconsin, 1989.

[4] —. Parabolic equations for curves on surfaces, II. Technical Report Technical Summary reports, 89-24, University of Wisconsin, 1989.

[5] A. Arehart, L. Vincent, and B. B. Kimia. Mathematical morphology: The Hamilton-Jacobi connection. In *ICCV4 (Germany, Berlin, May 11-13, 1993)*, Washington, DC, 1993. Computer Society Press.

[6] H. Asada and M. Brady. The curvature primal sketch. *IEEE PAMI*, 8:2–14, 1983.

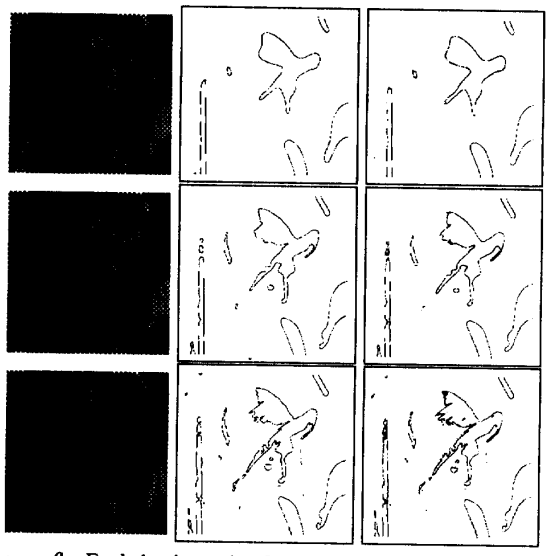

Figure 6: Each iso-intensity level set is smoothed independently of the rest of the image. LEFT COLUMN (bottom to top): The sequence of curvature deformation smoothed images. MIDDLE COLUMN (bottom to top): The level set (intensity = 125) of the smoothed image to the left is the evolution by curvature of the original image's level set (intensity = 125). RIGHT COLUMN (bottom to top): The evolution by curvature of the same level set, but with a different surface (obtained from the distance transform). Note the correspondence between the middle and right columns.

[7] J. Babaud, A. P. Witkin, M. Baudin, and R. O. Duda. Uniqueness of the gaussian kernel for scale-space filtering. *IEEE PAMI*, 8(1):26–33, January 1986.

[8] G. Barles. Remarks on a flame propagation model. Technical Report No 464, INRIA Rapports de Recherche, December 1985.

[9] H. Blum. Biological shape and visual science. *J. Theor. Biol.*, 38:205–287, 1973.

[10] F. Catté, P.-L. Lions, J.-M. Morel, and T. Coll. Image selective smoothing and edge detection by nonlinear diffusion. *SIAM Journal of Numerical Analysis*, 29(1):182–193, February 1992.

[11] Y. Chen, Y. Giga, and S. Goto. Uniqueness and existence of viscosity solutions of generalized mean curvature flow equations. *Journal of Differential Geometry*, 33(3):749–786, 1991.

[12] M. G. Crandall, H. Ishii, , and P.-L. Lions. User's guide to viscosity solutions of second order partial differential equations. *Bulletin of the American Mathematical Society*, 27(1):1–67, 1992.

[13] M. G. Crandall and P.-L. Lions. Viscosity solutions of Hamilton-Jacobi equations. *Trans. Amer. Math. Soc.*, 277:1–42, 1983.

[14] L. C. Evans and J. Spruck. Motion of level sets by mean curvature II. Technical report, University of Massachusetts at Amherst.

[15] —. Motion of level sets by mean curvature III. Technical report, University of Massachusetts at Amherst.

[16] —. Motion of level sets by mean curvature I. *Journal of Differential Geometry*, 33(3):635–681, May 1991.

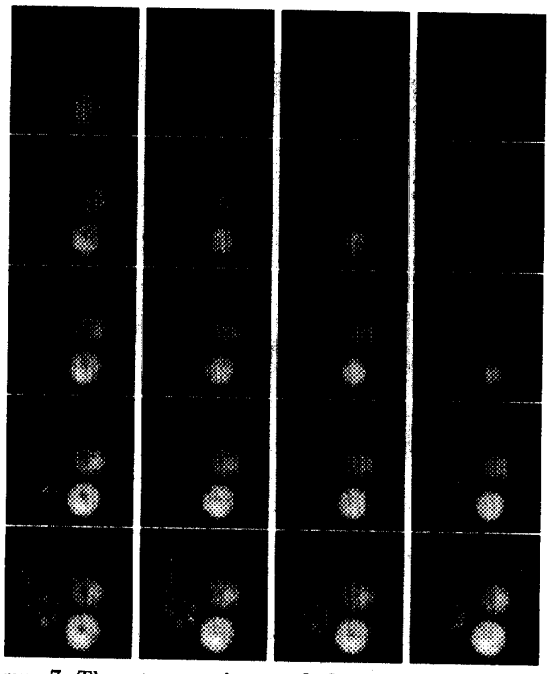

Figure 7: The entropy scale space [29] for the FRUITS image. LEFT COLUMN (bottom to top): Constant deformation only. LEFT TO RIGHT (bottom to top): Increasing amounts of curvature deformation. Whereas under curvature deformation all iso-intensity curves are smoothed to circles which eventually disappear, constant deformation leads to the "breaking off" of structures, *e.g.*, the grapes.

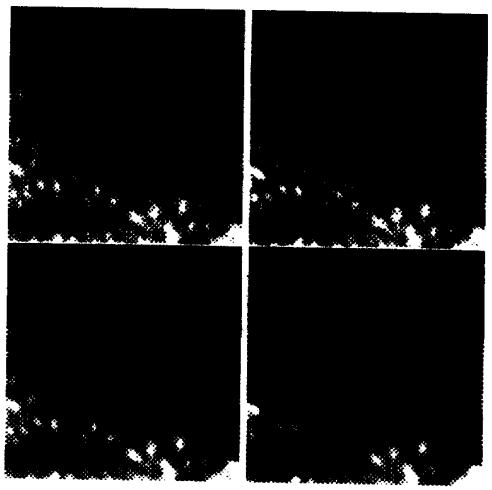

Figure 8: Curvature deformation smoothing for the BANDS image. CLOCKWISE FROM TOP LEFT: Curvature deformation eliminates noise and enhances the ocular dominance columns: slowly curving edges remain sharp while edges corresponding to smaller structures are removed.

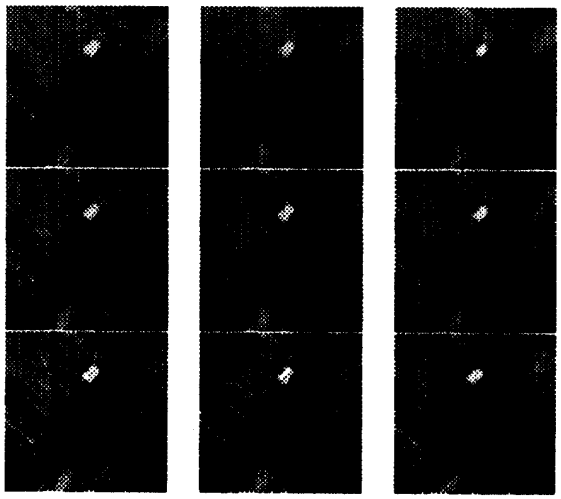

Figure 9: A comparison of curvature deformation and anisotropic diffusion [46] for the ROADS image. Anisotropic diffusion is applied with the conductance function $g(\nabla\phi) = 1/(1 + (|\nabla\phi|/K)^2)$. When g drops sharply with increasing image intensity gradient ($K = 5$, LEFT COLUMN), all sharp edges are preserved, including those of small structures such as the cars. When g is less steep ($K = 10$, MIDDLE COLUMN) small structures are smoothed over but so too are the slowly curving edges of larger structures such as the roads. Curvature deformation (RIGHT COLUMN) exhibits the property of smoothing over the small structures, while preserving the slowly curving contours of the roads.

[17] O. Faugeras, editor. Lecture Notes in Computer Science, 427. Berlin, 1990. Springer Verlag.

[18] M. Gage. An isoperimetric inequality with applications to curve shortening. *Duke Mathematical Journal*, 50:1225–1229, 1983.

[19] —. Curve shortening makes convex curves circular. *Invent. Math.*, 76:357–364, 1984.

[20] —. On an area-preserving evolution equation for plane curves. *Contemp. Math.*, 51:51–62, 1986.

[21] M. Gage and R. S. Hamilton. The heat equation shrinking convex plane curves. *J. Differential Geometry*, 23:69–96, 1986.

[22] M. A. Grayson. The heat equation shrinks embedded plane curves to round points. *J. Differential Geometry*, 26:285–314, 1987.

[23] E. Hopf. The partial differential equation $u_t + uu_x = \epsilon u_{xx}$. *Comm. Pure Appl. Math.*, 3:201–230, 1950.

[24] B. Horn and E. Weldon. Filtering closed curves. *IEEE PAMI*, 8(5), 1986.

[25] H. Ishii. On uniqueness and existence of viscosity solutions of fully nonlinear second-order elliptic pde's. 42:15–45, 1989.

[26] B. B. Kimia, A. R. Tannenbaum, and S. W. Zucker. Toward a computational theory of shape: An overview. CIM-89-13, McGill Centre for Intelligent Machines, McGill University, Montreal, Canada, 1989.

[27] —. Reaction-diffusion equations and shape. In *Proceedings of the British Conference on Computer Vision*, Britain, 1990.

[28] —. Toward a computational theory of shape: An overview. In Faugeras [17], pages 402–407.

[29] —. Entropy scale-space. In C. Arcelli, editor, *Visual Form: Analysis and Recognition*, pages 333–344, New York, May 1991. Plenum Press.

[30] —. Exploring the shape manifold: The role of conservation laws. In *Proceedings of the Shape in Picture NATO conference*, September 1992.

[31] —. On the evolution of curves via a function of curvature, I: The classical case. *JMAA*, 163(2), January 1992.

[32] —. The shape triangle: Parts, protrusions, and bends. Technical Report TR-92-15, McGill University Research Center for Intelligent Machines, 1992.

[33] —. Shapes, shocks, and deformations, I: The components of shape and the reaction-diffusion space. *International Journal of Computer Vision*, To Appear, 1992.

[34] —. Nonlinear shape approximation via the entropy scale space. In *Proceedings of the SPIE's Geometric Methods in Computer Vision II*, volume 2031, pages 218–233, San Diego, California, July 1993.

[35] J. J. Koenderink. The structure of images. *Biological Cybernetics*, 50:363–370, 1984.

[36] J. J. Koenderink and A. J. van Doorn. Dynamic shape. *Biological Cybernetics*, 53:383–396, 1986.

[37] P. D. Lax. *Hyperbolic Systems of Conservation Laws and the Mathematical Theory of Shock Waves*. SIAM Regional Conference series in Applied Mathematics, Philadelphia, 1973.

[38] T. Lindeberg. Scale-space for discrete signals. *IEEE PAMI*, 12(3):234–254, 1990.

[39] P. Lions. *Generalized Solutions of Hamilton Jacobi Equations*. Pitman, 1981.

[40] D. G. Lowe. Organization of smooth image curves at multiple scales. In *ICCV2 (Tampa, FL, December 5–8, 1988)*, pages 558–567, Washington, DC,, 1988. Computer Society Press.

[41] H. Matano. Non-increase of the lapnumber of a solution for a one dimensional semilinear parabolic equation. *J. Fac. Sci. Univ. Tokyo IA Math.*, 29:401–441, 1982.

[42] F. Mokhtarian and A. Mackworth. Scale-based description of planar curves and two-dimensional shapes. *IEEE PAMI*, 8:34–43, 1986.

[43] —. A theory of multiscale, curvature-based shape representation for planar curves. *IEEE PAMI*, 14(8):789–805, August 1992.

[44] J. Oliensis. Local reproducible smoothing without shrinkage. *IEEE PAMI*, 15(3):307–312, March 1993.

[45] S. Osher and J. Sethian. Fronts propagating with curvature dependent speed: Algorithms based on hamilton-jacobi formulations. *Journal of Computational Physics*, 79:12–49, 1988.

[46] P. Perona and J. Malik. Scale-space and edge detection using anistropic diffusion. *IEEE PAMI*, 12(7):629–639, July 1990.

[47] M. H. Protter and H. F. Weinberger. *Maximum Principles in Differential Equations*. Springer-Verlag, New York, N. Y., 1984.

[48] K. Siddiqi and B. B. Kimia. Entropy scale space for images. Technical Report In Preparation, LEMS, Brown University, 1993.

[49] R. T. Whitaker and S. M. Pizer. A multi-scale approach to nonuniform diffusion. *CVGIP*, 57(1):99–110, January 1993.

[50] B. White. Some recent developments in differential geometry. *The Mathematical Intelligenecer*, 11(4):41–47, 1989.

[51] A. P. Witkin. Scale-space filtering. In *Proceedings of the* 8^{th} *International Joint Conference on Artificial Intelligence*, pages 1019–1022, Karlsruhe, West Germany, August 1983.

[52] A. L. Yuille and T. A. Poggio. Scaling theorems for zero crossings. *IEEE PAMI*, 8(1):15–25, January 1986.